(12)

REPORT HLD-82-1R

HELIONETICS, INC.
LASER DIVISION

INTERIM TECHNICAL REPORT
AND R & D STATUS REPORT

OPTIMIZATION OF EFFICIENCY OF A DISCHARGE-EXCITED XeCl LASER

CONTRACT N00014-82-C-0087

MARCH 1982

BY

HELIONETICS, INC.
Laser Division
3878 Ruffin Road
San Diego, CA 92123

Prepared for

OFFICE OF NAVAL RESEARCH
800 North Quincy Street
Arlington, Virginia 22217

R & D STATUS REPORT and
INTERIM TECHNICAL REPORT

ARPA Order No. 4370 Program Code NR 428-004
Contractor: HELIONETICS, INC., LASER DIVISION
3878 Ruffin Road, San Diego, CA 92123

Contract No. N00014-82-C-0087
Contract Amount: $699,000.00

Effective Date of Contract: 22 October 1981
Expiration Date of Contract: 21 October 1982

Principal Investigator: Dr. D.E. Rothe
Telephone No. (714) 560-6273

TITLE: OPTIMIZATION OF EFFICIENCY OF A DISCHARGE-EXCITED XeCl LASER

Reporting Period: 22 October 1981 - 21 February 1982

SECURITY CLASSIFICATION OF THIS PAGE (When Data Entered)

REPORT DOCUMENTATION PAGE

READ INSTRUCTIONS BEFORE COMPLETING FORM

1. REPORT NUMBER	2. GOVT ACCESSION NO. AD-A112107
	3. RECIPIENT'S CATALOG NUMBER
4. TITLE (and Subtitle) Optimization of Efficiency of a Discharge-Excited XeCl Laser	5. TYPE OF REPORT & PERIOD COVERED Interim Technical Report 22 Oct.1981 -21 Feb.1982
	6. PERFORMING ORG. REPORT NUMBER HLD - 82 - 1R
7. AUTHOR(s) D. E. Rothe	8. CONTRACT OR GRANT NUMBER(s) N00014-82-C-0087
9. PERFORMING ORGANIZATION NAME AND ADDRESS Helionetics, Inc. 17312 Eastman Street Irvine, California 92714	10. PROGRAM ELEMENT, PROJECT, TASK AREA & WORK UNIT NUMBERS
11. CONTROLLING OFFICE NAME AND ADDRESS Office of Naval Research 800 North Quincy Street Arlington, VA 22217	12. REPORT DATE March 1982
	13. NUMBER OF PAGES
14. MONITORING AGENCY NAME & ADDRESS(if different from Controlling Office) Defense Contract Administration Services 34 Civic Center Plaza P. O. Box C-12700 Santa Ana, California 92712	15. SECURITY CLASS. (of this report) Unclassified
	15a. DECLASSIFICATION/DOWNGRADING SCHEDULE

16. DISTRIBUTION STATEMENT (of this Report)

Approved for Public Release; Distribution unlimited

17. DISTRIBUTION STATEMENT (of the abstract entered in Block 20, if different from Report)

None

18. SUPPLEMENTARY NOTES

None

19. KEY WORDS (Continue on reverse side if necessary and identify by block number)

Electric-Discharge Excited XeCl Laser, X-Ray Preionization, Water Blumlein, Efficient Energy Transfer.

This work supports the

20. ABSTRACT (Continue on reverse side if necessary and identify by block number)

The work reported here is in support of the U.S. Navy's strategic blue-green laser communication program. The specific goal ~~of the present effort~~ is to raise the efficiency of an electric-discharge-excited XeCl laser to 3% or better. Efficient XeCl lasers are prime candidates for a satellite-borne laser transmitter.

During the first four months of this contract, the design, construction and assembly of a versatile XeCl laser test bed has been (completed. Initial checkout and performance tests are in progress.) Without optimization of the pulse-forming-network, optical cavity and gas mixture, the laser has produced optical pulses with energies in excess of 1 joule with efficiencies over 1%. Prospects for raising these characteristics to 2 joules and 3% with proper optimization and injection locking are very good.

was

DD FORM 1 JAN 73 1473 EDITION OF 1 NOV 65 IS OBSOLETE

SECURITY CLASSIFICATION OF THIS PAGE (When Data Entered)

TABLE OF CONTENTS

1.0 SUMMARY

The work reported here is in support of the U.S. Navy's strategic blue-green laser communication program. The specific goal of the present effort is to raise the efficiency of an electric-discharge-excited XeCl laser to 3% or better. Efficient XeCl lasers are prime candidates for a satellite-borne laser transmitter.

During the first four months of this contract, the design, construction and assembly of a versatile XeCl laser test bed has been completed. Initial checkout and performance tests are in progress. Without optimization of the pulse-forming-network, optical cavity and gas mixture, the laser has produced optical pulses with energies in excess of 1 joule with efficiencies over 1%. Prospects for raising these characteristics to 2 joules and 3% with proper optimization and injection locking are very good.

2.0 INTRODUCTION

In this section the unique advantages of a Pb-vapor Raman shifted XeCl Laser as a transmitter for "submarine laser communications" (SLC) are reviewed.

For a satellite-based transmitter (SLC-SAT) the minimum laser specifications, consistent with a projected data rate of information transmission over a specified area of ocean surface, are as follows:

Optical Pulse Energy	> 2 J
Wavelength	450-500 nm
Bandwidth	< 1 A
Pulse Repetition Frequency (PRF)	100 Hz
Pulse Duration	50-500 ns
Transmitter Efficiency	> 1 %
Reliability	Space Qualifiable
Life	3 Years (10^{10} pulses)

The transmitter efficiency is of paramount importance here because of the limited amount of electrical power that can be generated by photovoltaic solar panels or by nuclear power cells on the satellite.

At the present state of laser technology, only two types of laser transmitter are considered seriously as having the potential to produce the required pulse energy and average power at an overall efficiency of well over 1%, while having a projected maintenance-free life of several years. These are the electric-discharge-excited HgBr laser, which lases in the blue-green band directly (503 nm), and the XeCl laser (308 nm) coupled with a highly efficient Raman down-converter for shifting the ultraviolet laser output to the blue-green region (459 nm). Raman down-conversion in lead vapor with close to 50% energy conversion efficiency has already been obtained[1]. Even though the demonstrated XeCl laser efficiency[2] of 2.1% is higher than the 1.4% efficiency obtained with a HgBr laser[3], the Raman down-conversion makes the XeCl/Raman

---

1. Recent results obtained at NRTC and NRL

2. NRTC 1981

3. MSNW 1981

system only 2/3 as efficient as the HgBr laser system. As a consequence, the Navy has elected to pursue only the HgBr laser system through the breadboard stage, until such time as an equivalent high efficiency can be demonstrated with another blue-green laser (such as the XeCl/Pb-vapor Raman). Efforts to demonstrate greater than 3% efficiency with a discharge-pumped XeCl laser are underway at Helionetics as part of this contract.

The HgBr laser is very sensitive to quenching by impurities in the gas mixture. This in combination with the extreme corrosion and alloying problems associated with hot mercury and bromine compounds makes the HgBr laser a very difficult device to engineer. Contamination and materials problems are much less severe for an XeCl laser.

Furthermore, it must be kept in mind that the effectiveness of laser submarine communications does not only depend on the laser signal strength (proportional to transmitter efficiency for a given input power), but also on the efficiency of the detector for discriminating signal against background noise (skylight and direct sunlight).

The ideal receiver appears to be the quantum-limited optical resonance detector (QLORD) recently invented by Marling[4]. Some of the advantages of the QLORD over other narrow-band filters are:

1. Extremely narrow spectral acceptance bandwidth ($\approx$ 0.01A)
2. High signal-to-noise discrimination (10^5 - 10^6)
3. Wide acceptance angle (2π steradian)
4. High photon transmission factor (0.9)
5. Low manufacturing cost.

Basically, the QLORD consists of a glass cell filled with an alkali vapor which has a resonant absorption line at the transmitter frequency in the blue-green. The absorbed blue-green energy is then reradiated as infrared and near-infrared photons. The latter are detected by a bank of photomultiplier tubes. Highly efficient broadband filters are employed to prevent near-infrared light from entering the cell and to permit none but near-infrared photons to pass from the cell to the detectors. Light can thus enter the photomultipliers only via the resonance lines at 459.3 nm and 455.5 nm with a total acceptance bandwidth of only 0.036 A.

---

4. J.B. Marling, J Appl. Phys. 50, 610 (1979

Due to a fortuitous coincidence, the lead-vapor Raman-shifted XeCl laser can be tuned[5] to emit at the 459.3 nm resonance line of cesium. No such concidence has been found between the HgBr laser emission and the absorption of any suitable atomic vapor for a corresponding QLORD. This circumstance makes the XeCl-laser/Pb-vapor Raman/QLORD very unique and gives it a decisive advantage over other competitive blue-green SLC systems.

A recent study[6] by independent consultants to Helionetics has shown that the system efficiency for the transmitter-detector combination is considerably higher (by 2 orders of magnitude) for the XeCl/Pb-Raman/Cs-QLORD system than it is for the competitive HgBr/Lyot Filter. This analysis indicates that the XeCl/QLORD system can successfully communicate with submarines which are up to twice as deep as permissible with the corresponding HgBr/Lyot Filter system. The signal-to-noise ratio is compared for the two systems as a function of submarine depth and class of seawater in Figure 1 (equal transmitter pulse energies were assumed in the study).

5. R. Burnham, Reported in Tech. Doc. 352, "Strategic Laser Communications Program", Vol.1, Proc. Navy/DARPA 4th. Tech. Interchange Mtg., NOSC, San Diego, CA (1980) P. 171.

6. R.N. Keeler and J.B. Marling, "The Applicability of the XeCl laser and the Cesium QLORD to Submarine Communications" Helionetics, Inc., San Diego, CA. (White Paper submitted to ONR, December 1981).

3.0 APPROACH FOR INCREASING XeCl LASER EFFICIENCY

This section reviews the various considerations that influenced the design of the XeCl laser test bed.

3.1 Energy Flow in a Discharge-Excited XeCl Laser

The energy flow in a typical discharge-pumped XeCl laser is shown in Figure 2. The first three steps involve the power conditioning process, going from DC power to capacitor to pulse-forming-network (PFN) to the discharge. In this process the DC power is transformed into discrete energy pulses, which are delivered to the discharge (load) with a predetermined and optimized voltage and current pulse waveshape.

In the first step, electrical power is transferred to a capacitor which is charged inductively (as opposed to resistive charging for which the power loss is 50%) in a time scale consistent with the time between laser pulses (i.e. in 10 ms for a 100 Hz machine). The technology for this step is well developed, so that this energy transfer can be accomplished by inductive charging (e.g. with a resonant charging choke or with a saturable-core reactor) with approximately 98% efficiency.

The second step involves the transfer of energy from the capacitor to a pulse-forming-network (in our case a water Blumleim configuration), which is designed to produce the desired pulse shape. This transfer can be accomplished on a microsecond scale with peak currents on the order of 1000 A. Efficient thyratron switches have been developed for Radar-type pulsed power applications with almost exactly the same type of voltage, current and di/dt requirements. The technology for performing step 2 efficiently is therefore readily available. An energy transfer efficiency of approximately 95% for this step can easily be achieved (inclusive of the power requirements for heating the thyratron cathode and hydrogen reservoir, which may be as high as half a kilowatt).

The pulse-forming-line is designed to produce voltage and current pulseshapes which optimize the amount of energy desposited in the gas during the discharge pulse. For maximum power transfer, the line impedance should be closely matched to the discharge impedance. To a first approximation, a high-pressure glow discharge acts as a constant-voltage load (just as the normal low-density glow); so that the discharge impedance is approximately inversely proportional to the current supplied by the PFN (for a given gas mixture, pressure and discharge electrode seperation). Impedance matching is achieved when the open-circuit line (generator) voltage is twice the discharge voltage. In principal, it should thus be easy to achieve perfect energy transfer to the discharge with a constant-voltage, constant-current pulse-forming line by simply adjusting the supply voltage and/or the gas pressure or electrode separation (for a constant E/N discharge, the discharge voltage is proportional to the gas density and the electrode separation) until the generator/load voltages and impedances are matched.

In practice, this situation is complicated by at least two effects:

1. Discharge instabilities drive the discharge impedance down to a low value.

2. The discharge formation time (inversely proportional to the electron avalanche multiplication rate) may take up a substantial fraction of the pump pulse duration supplied by the PFN.

If discharge instabilities, in the form of a bulk ionization runaway or a localized glow-to-arc transition, develop during the discharge pulse, the discharge impedance can vary over a wide dynamic range during the pulse. As a consequence, effective impedance matching and effective energy transfer are not possible under such conditions. Ionization runaway can be avoided by working with gas mixtures rich in electron-attaching species (F_2, HCl etc.). Arc instabilities can be prevented from developing (at least during the first few hundred nanoseconds) by initiating the discharge in as volumetrically uniform a manner as possible. This requires:

1. Uniform pre-discharge field (uniform to within a few percent).

2. Uniform preionization at a level of 10^6 to 10^9 electrons per cm^3 (uniform to within a few percent).

3. Fast voltage rise at the discharge electrodes (rise time of 10 ns or less)[7]

Whereas the problems associated with discharge instabilities are very complex and not too well understood, pulsed gas laser technology has developed to the stage where relatively stable discharges can be produced and maintained for hundreds of nanoseconds.[8]

The avalanche discharge formation time may be a more serious obstacle in preventing the efficient transfer of electrical energy to the discharge. When the voltages and impedances are closely matched, the avalanche formation times can be quite long (30 to 100 ns). Conversely, the supply voltage must be raised substantially over the discharge sustaining voltage to bring the discharge formation time down to a few nanoseconds. This problem is discussed in more detail in Section 3.3.

---

7. J.I. Levatter and S.C. Lin, J. Appl. Phys. 51, 210 (1980).

8. J.I. Levatter, "A Review of Engineering Considerations and Recent Experimentation Regarding an X-Ray Preionized Avalanche Discharge Excimer Laser," Electro-Optics/Laser 80 Conference, Boston, Mass. (Nov. 19-21, 1980)

In view of the above considerations, the energy transfer from the PFN to the discharge is less than perfect, and may range from less than 40% to 80%. The energy transfer must be accomplished with a fast, low-inductance switch capable of a dV/dt and di/dt of 10^{13} V/s and 10^{13} A/s respectively in order to achieve the 10 ns voltage rise necessary for discharge stability. Helionetics has developed a triggered multichannel rail gap, which can easily be adapted to a parallel-plate Blumlein PFN and which conforms to the above requirements. Such a switch is used in the present program to discharge the PFN.

Only part of the energy deposited by the discharge in the gas ends up in producing a population of XeCl* excited states (upper lasing level). The excited-state production efficiency (η_4) is a function of the discharge kinetics and the chemical kinetic processes occuring in the gas mixture.

The discharge kinetics deal with the energy transfer between the discharge electrons and the primary gas compounds (Xe, HCl and the diluent, i.e. He or Ne). Both elastic and inelastic collisions occur in the gas, and the electron energy distribution ends up being non-Maxwellian. Energy transfer by elastic collisions manifests itself as heating of the gas, whereas inelastic collisions lead to the production of excited atoms and molecules (Xe^*, Ne^*, He^*, HCl^*) and ions (Xe^+, HCl^-). At the E/N values of a typical gaseous discharge, (E/N value is a function of gas mixture ratio only) a relatively large fraction of the electron energy goes into heating of the diluent gas. At higher E/N values the production efficiency of metastables and ions would be higher. Additives, which raise the E/N value of the discharge, would therefore be beneficial, provided the additives do not lead to the formation of species which absorb the laser radiation or which act as quenchants to the laser kinetics.

The chemical kinetics deal with the excited-state chemistry and ion recombination reactions which lead to the production of XeCl* and various other species. XeCl* may be produced by reactions of metastables (Xe^*, Xe_2^*, $XeNe^*$) with HCl or Cl (Neutral formation channel) or by Xe^+, Xe_2^+ and $XeNe^+$ ions recombining with HCl^- or Cl^- (Ion channel). Both formation channels are believed to be important, with the ion channel dominating.

After taking into account the power partitioning in the discharge and accounting for the competition between various chemical reactions and their branching ratios, predicted excited state production efficiencies are typically between 10 and 15%. Since the chemical kinetics cannot be optimized independently (e.g. gas mixtures and conditions, which optimize the production of XeCl*, may lead to discharge instabilities or the production of optical absorbers), realistic excited-state production efficiencies have been assumed to be in the 6 to 13% range.

Once a population of XeCl* has been established in the discharge volume, the excited-state energy has to be extracted by stimulated emission in an optical resonator to produce the laser pulse. The steady-state optical power extraction efficiency is directly related to the optical gain/absorption ratio. Known optical absorbers are Xe_2^+ (photodissociation) and Cl^- (photodetachment).

In addition to the steady-state extraction losses, a significant amount of optical energy may be lost at the beginning of the pulse, because the wave intensity in the resonator takes a finite time to build up to the saturation value. During this period the stimulated emission is in strong competition with spontaneous emission and collisional quenching. Quenched lifetime of XeCl* is typically about 10 ns.

The buildup period can be considerably reduced by ensuring a fast rise in pump power to lasing threshold. This implies a fast discharge current rise and requires a low discharge-chamber inductance. Furthermore, the optical oscillation buildup (which normally starts out from spontaneous "noise") can be speeded up significantly (by approximately 20 ns) by injection locking. Injection locking has the additional advantage of preventing oscillation on parasitic modes.

With absorption being a few percent per cm and without injection locking, typical extraction efficiencies are around 50%. With high values of gain/absorption ratio, fast current rise, and injection locking of the optical cavity, it may be possible to raise the extraction efficiency into the 70 to 80% range.

As shown in Figure 2, the overall laser efficiency is the product of all the energy transfer efficiencies, the excited-state production efficiency and the optical extraction efficiency. For the practical ranges of efficiency values indicated, overall laser efficiency may range from less than 1% to as high as 7%.

Highest laser efficiency obtained so far with a discharge-excited XeCl laser was 2.1% (demonstrated in 1981 by Northrop), with estimated efficiency factors of $\eta_3 = 0.42$, $\eta_4 = 0.09$ and, $\eta_5 = 0.56$. Using these numbers as a baseline, possible improvement factors are 1.90 for the energy transfer from the PFN to the discharge, 1.44 for laser kinitics, and 1.43 for the optical extraction (see Table 1). As can be seen from this comparison, the highest gain can be made by maximizing the energy transfer to the gas. Hence, the present program concentrates heavily on the PFN technology and discharge physics.

3.2 Optimization of Design Parameters

The approach for increasing laser efficiency addresses all three areas: energy transfer, laser kinetics and optical extraction. The technical design considerations, which are consistent with improving the various aspects of the discharge-pumped laser, are outlined in Tables 2 and 3.

To facilitate operating the laser over as wide a range of gas mixture ratio, gas pressure and pump power density as possible, every effort is made here to maximize the discharge stability. Uniform preionization is provided by an x-ray source. Fast voltage rise at the discharge electrodes is achieved by employing a low-inductance fast multichannel rail gap as the switch for discharging the PFN. A short resistive switch-closure phase is obtained by choosing an electrode design and triggering mode which promote spark breakdown in many parallel arc channels. A pulse-sharpening rail gap is used to decrease the voltage risetime at the discharge electrodes further to approximately 3 ns. Power losses in the switches may be reduced by using hydrogen instead of air in the spark gaps.

For optimum energy transfer, the PFN and discharge impedances will be operated in as close a matched condition as permissable in terms of overvolting the discharge gap sufficiently for fast avalanche formation. In order to achieve high discharge sustaining voltages, it is best to work with large electrode separations and high pressures (6 to 10 atm).

For minimizing the pump-power build-up losses a large di/dt is required. Since this is proportional to L/Z, it is important to keep the discharge-chamber inductance as small as possible (<5nH), and to keep the pulse-forming line impedance moderately high (> 0.5Ω). Use of a double-sided transmission line drive reduces the chamber inductance by a factor of one half. A long pump pulse duration (100 ns) will also help in reducing the fractional energy loss due to power build-up.

Good discharge stability will make it easier to optimize the discharge kinetics and laser kinetics. It may facilitate the use of gas diluents which provide a larger fraction of high-energy electrons in the discharge. Empirically XeCl lasers working with neon diluents have shown almost twice the efficiency than lasers operating on a corresponding helium mixture. Consequently, the baseline mixture for the present experiments will be a neon mixture at approximately 6 atmospheres. Recent calculations[9] have indicated that XeCl laser efficiency can be increased by pumping the gas harder, at a level of several MW/cm^3. High power density implies a relatively small discharge volume.

Optical extraction losses can be minimized by injection locking, which serves to speed-up the optical oscillation build-up and to eliminate parasitic oscillations.

3.3 XeCl Laser Design and Experimental Arrangement

The somewhat unique features which were incorporated into the design of the XeCl laser test setup are:

1. Minimized loop inductances for discharge chamber and rail gaps.
2. Use of pulse-sharpening rail gap in addition to triggered rail gap.
3. Moderately large line impedances.
4. Rail gaps twice as long as discharge.
5. Use of a double blumlein drive matched to a variable - taper double transmission line.
6. Laser head and spark gaps designed to accommodate wide ranges of gas mixture ratios and gas pressures.
7. X-ray preionizer
8. Frequency - doubled dye laser for injection locking.

---

9. S. C. Lin, UCSD, San Diego, Cal., private communication (1981)

The PFN for this laser has been intentionally designed with a 2:1 mismatch between the pulse-forming line impedance and the expected discharge impedance. This is a compromise between achieving optimum power transfer during the discharge pulse and generating a sufficient overvoltage, so that the avalanche formation time τ_A makes up a small fraction of the generated pulse duration τ_p.

The reasons for this choice can be illustrated in quantitative terms by considering the energy transfer to the discharge as a function of overvoltage (or degree of impedance mismatch). We begin by defining a voltage ratio ϕ as being the ratio of the open-circuit generator (here a double-Blumlein) voltage divided by the steady-state discharge voltage V_D. For the Blumlein configuration (Figure 3):

$$\phi = 2V_{CH}/V_D, \text{ where } V_{CH} = \text{charging Voltage}$$

The impedance ratio between line impedance Z and discharge resistance R is then:

$$Z/R = \phi - 1$$

and the energy transfer efficiency (assuming $\tau_A \ll \tau_p$) is

$$\eta_3 = 4(\phi-1)/\phi^2$$

Avalanche formation times have recently been calculated[10] for a $He/Xe/F_2$ mixture and are tabulated in Table 4 as a function of ϕ. Note that for the impedance-matched condition (Z=R and ϕ=2) the avalanche formation time is 35 ns, which is a substantial fraction of τ_p, if the pulse generated is 100 ns long. The avalanche formation time τ_A can be considerably reduced (to 8 ns), however, by going to a 3:1 voltage ratio, while at the same time keeping the energy transfer reasonably high (89% during discharge). For higher voltage ratios the energy transfer rapidly declines (e.g. for ϕ=10, η_3 = 0.36). Even though the calculations were performed for an XeF laser mixture, the trend noted here is expected to be very similar for an XeCl laser mixture. As part of this program, the existing UCSD code will be applied to generating theoretical values for a typical Ne/Xe/HCl mixture.

Table 5 shows the chosen laser design specifications and the baseline conditions for the discharge and PFN. The design gas mixture is Ne/Xe/HCl = 97.8/2.0/0.2 at 6 atm total pressure. Nominal discharge voltage is 27 kV based on an E/N-value of 4.7×10^{-17} V-cm^2. The electrode separation is 3.6 cm, and the discharge volume is 324 cm^3. At a charging voltage of 40.5 kV (ϕ=3), the energy stored in the PFN is 75 J. This translates to an energy density deposited in the gas of 35 J/l-atm and a power density of 2 MW/cm^3. The lengths of the Blumlein plates are chosen to give a 100 ns pulse duration. The pulse-forming line impedance is 2 ohm, but can easily be changed to a lower value.

---

10. H.H. Luo, Ph.D. thesis, University of Calif., San Diego (1978)

The overall experimental arrangement is shown in Figure 4. Note, the tunable dye laser and frequency doubler for injection locking and for gain and absorption measurements. The x-ray generator, used for preionization of the gas mixture, requires less than 1% of the total power input. Its use does therefore not appreciably affect the laser efficiency. The trigger pulses T_1 to T_4 have to be applied in the proper time sequence for the system to operate correctly. T_1 initiates the pulse charging of the PFN from a conventional capacitor. T_2 triggers the rail gap which discharges the pulse-forming line into the laser gas. T_3 initiates a plasma at the e-beam cathode of the x-ray generator which turns on the e-beam (i.e. x-ray flux). T_4 fires the flash lamps which energize the dye laser. Timing of the trigger pulses is adjusted, so that the frequency-doubled dye laser beam and the x-ray flux pass through the laser cavity before and during the initiation of the electric discharge.

The construction of the discharge chamber is shown in cross-section in Figure 5. The chamber is designed for low inductance (3.5 nH) and high pressure (up to 20 atm). The chamber is machined into a relatively massive aluminum block (nickel plated for compatibility with the stainless steel water Blumlein). The anode insulator is machined out of a single Kynar block and is subjected to compressive stresses only (no bending, tension or shear). The insulator extends into the chamber to form antitracking barriers.

The discharge cross-section (and beam cross-section) is nominally 1.8 cm wide and 3.6 cm high. The electrodes are made from 6061 aluminum alloy and are contoured according to a compacted Chang[11] electrode profile. The central section of the anode is hollowed out (leaving a 2 mm thick shell) to permit the preionizing x-rays to pass into the discharge volume. The anode feedthrough and the clamping blocks holding it in place are made from stainless steel.

The physical geometry of the pulse-forming line is depicted in Figure 6. Note the location of the triggered rail gap (SW1) at the end of the parallel-plate double Blumlein. The double Blumlein is impedance-matched to a variable-taper double transmission line. The pulse-sharpening slave rail gap (SW2) is located between the Blumlein and the transmission line section. The slave gap is removable, in case the energy losses in the gap exceed the benefits derived from the faster voltage rise produced by the gap.

---

11. T. Y. Chang, Rev. Scient. Inst. 44, 405 (1973)

The pulse-charging circuit for energizing the PFN is shown in Figure 7. Pulse charging time is 2 μs with L_1 = 9 μH as shown, or 1 μs when L_1 = 2 μH. The 90 nF capacitor is equal to the 2 ohm double Blumlein capacitance. At present a single-channel spark gap is used to transfer the electric charge from the capacitor to the PFN (with an approximately 20% energy loss).

An "equivalent" discrete-component ircuit of the electric pulser is given in Figure 8. Note the location of the rail gaps. The Blumlein corresponds to a 2-stage LC-voltage-doubler, and the transmission line section corresponds to a 4 nF peaking capacitor. The charging resistors, R_1 and R_2, are the resistances of the water between the PFN plates, based on a resistivity of 10 Megohm-cm.

4.0 PROGRESS

Progress on this program has been substantially faster than originally anticipated. This occurred as a result of a concentrated effort to compress a 12 month program into a six to eight month schedule.

4.1 Accomplishments During First Four Months of Program.

During this reporting period, the basic laser system has been designed, built and assembled. All components shown in Figure 4 are complete; except the frequency-doubled dye laser has not been incorporated into the setup. A pictorial view of the XeCl laser with pulse-forming line, pulse-charging section, x-ray generator, power supplies, control consoles, trigger pulse generators and instrumentation is afforded in Figure 10.

The laser test setup may be broken down into various subsystems as follows:

1. Discharge chamber and electrodes
2. Pulse-forming line and rail gaps
3. Pulse-charging circuit
4. Trigger and timing circuits
5. X-ray preionizer
6. Optical cavity

Subsystems 1 to 4 have been described in some detail in the previous section.

The x-ray generator was designed and built by Beta Development Corp. (Model No. 80-1) to conform with the specific requirements for this program. It utilizes backward-emitted x-rays from a tantalum e-beam anode, which is in the center of a 12 inch diameter stainless-steel tube. The e-gun cathode is a surface-spark plasma array which can be moved relative to the anode. Anode-cathode spacing can be adjusted between 3 cm and 8.5 cm. The e-gun can be operated with anode voltages between 50 kV and 120 kV. The e-beam pulse energy is provided by the electric charge stored in a 6 m length of high-voltage cable, which is DC charged to the accelerating potential. The e-beam is switched on by pulsing the spark array. E-beam (and x-ray) pulse duration is between 60 ns and 150 ns, depending on A-K spacing. At a charging voltage of 100 kV and an A-K spacing of 3 cm the current density at the e-beam anode is approximately 5 A/cm^2 (1.5 A/cm^2 at an A-K spacing of 8.5 cm). Uniformity of the x-ray flux at the x-ray window has been measured to be within ±10% over the 60 cm long aperture. The e-beam energy per pulse is less than 1 joule.

For the first series of tests, in which the PFN and discharge parameters are optimized, the optical cavity will consist of externally mounted reflectors, forming a plane-parallel or concave (10 m R. of C.)-plane stable resonator. Output couplers with 10, 20, 30 and 40% reflectivity are available. The discharge chamber is sealed with near-normal anti-reflection-coated quartz windows.

Optics have been acquired for two types of unstable resonator configurations which permit injection locking. These are:

1. Edge-coupled Output. This resonator is a conventional confocal positive-branch unstable configuration. Mirrors have totally reflective coatings. Round-trip magnification is 3, with an effective output coupling of 79%. The concave mirror has a 1 mm x 2 mm hole for injecting the control signal from the dye laser. The convex output coupler has a reflective rectangular spot of 6 mm x 12 mm.

2. Continuously-coupled output. This is a hybrid confocal resonator. Round-trip magnification is 1.25. Both mirrors are coated over their entire surfaces with partially reflective multilayer dielectric coatings. The concave reflector is 97% reflective. The injected signal will be coupled in through this reflector. The convex mirror has a 20% reflective coating (at 308 nm) and serves as the output coupler. Total cavity loss is calculated to be 83%, of which 90% are extracted as a useful output beam through the convex mirror.

4.2 Initial Check-Out of Laser

The initial check-out and performance tests of the laser system are in progress. No injection locking has been attempted, and the PFN, laser gas and optical cavity have not been optimized. Nevertheless, XeCl laser pulses of more than 1 J energy have been measured with a system efficiency exceeding 1%.

All subsystems appear to perform as expected. No surface tracking has been observed in the laser chamber with conventional laser mixtures. The PFN has been tested at charging voltages up to 50 kV without water breakdown. The x-ray generator has been tested up to 110 kV. Jitter and timing considerations associated with firing the thyratrons and spark gap switches appear not to be a problem.

The triggered rail gap multichannels very nicely (approximately 50 arc channels) and exhibits a 10 ns voltage fall-time in the triggered mode of operation (see Figure 10A). Voltage fall-time for the same gap is 20 ns in the self-breakdown mode (Figure 10B). At present the PFN is inductively charged in 1 μs, and the rail gap is triggered at the peak of the sinusoidal charging voltage pulse. The voltage across the slave rail gap shows a 3 ns closure time (Figure 11). The voltage risetime at the discharge electrodes appears to be 8 ns, although the measured voltage waveform is very noisy at present and is suspect. All voltage measurements are performed with Pearson-type current monitors around purely resistive shunt loads.

5.0 STATUS OF WORK PERFORMED

At this point in time, the percent completion of the various tasks in this contract is as follows:

Task 1: Design, Fabrication and Test of a 2 J/Pulse Discharge-Pumped XeCl Laser

90% Complete

Task 2: Laser Output Diagnostics

30% Complete

Task 3: Modelling

0% Complete

Task 4: Laser Performance Optimization and Injection Locking

5% Complete

6.0 PLAN FOR OPTIMIZATION OF LASER

During the next month a systematic effort will be made to improve the energy transfer to the discharge. This includes the following items:

1. Improvement (cleanup from electric noise) of electrical and optical diagnostics.

2. Optimization of electrode profile and surface texture for most uniform discharge.

3. Lowering of the line impedance for better match to discharge impedance (Preliminary measurements indicate that discharge impedance is significantly lower than anticipated).

4. Increasing of power density and current density in the discharge. This will result in a faster gain buildup and may push the glow into the abnormal glow regime where the E/N value is significantly higher.

5. Parametric study of the efficiency as a function of gas mixture, pressure, charging voltage, and optical output coupling.

6. Study of the effects of the slave gap on optical output.

7. Kinetics calculations and modelling of the discharge and circuit will be initiated, using the kinetics code developed by S.C. Lin at University of California at San Diego.

Subsequently, the frequency-doubled dye laser (tunable Candela Model SLL-625A dye laser with etalon and ADP second harmonic generator) will be assembled and incorporated into the test setup. At first the dye laser will be used to probe the small-signal gain and absorption as a function of time to generate support data for the modelling studies. Later, the dye laser will be employed to injection-lock and frequency-narrow the XeCl laser.

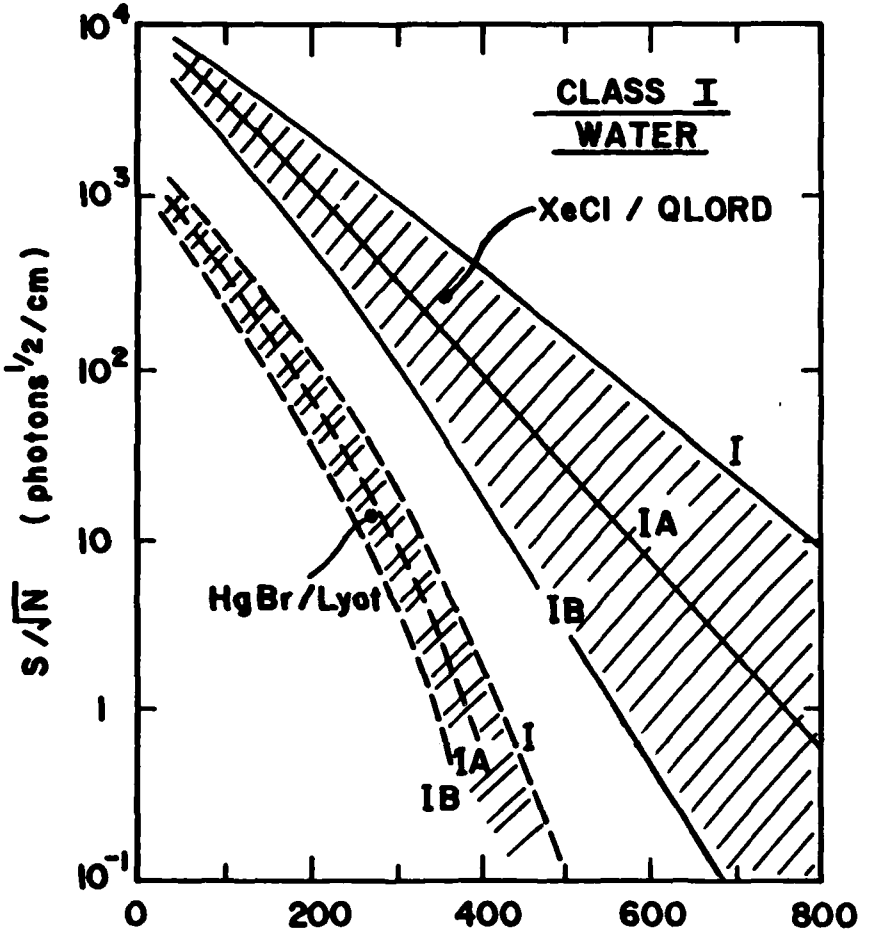

FIGURE 1A

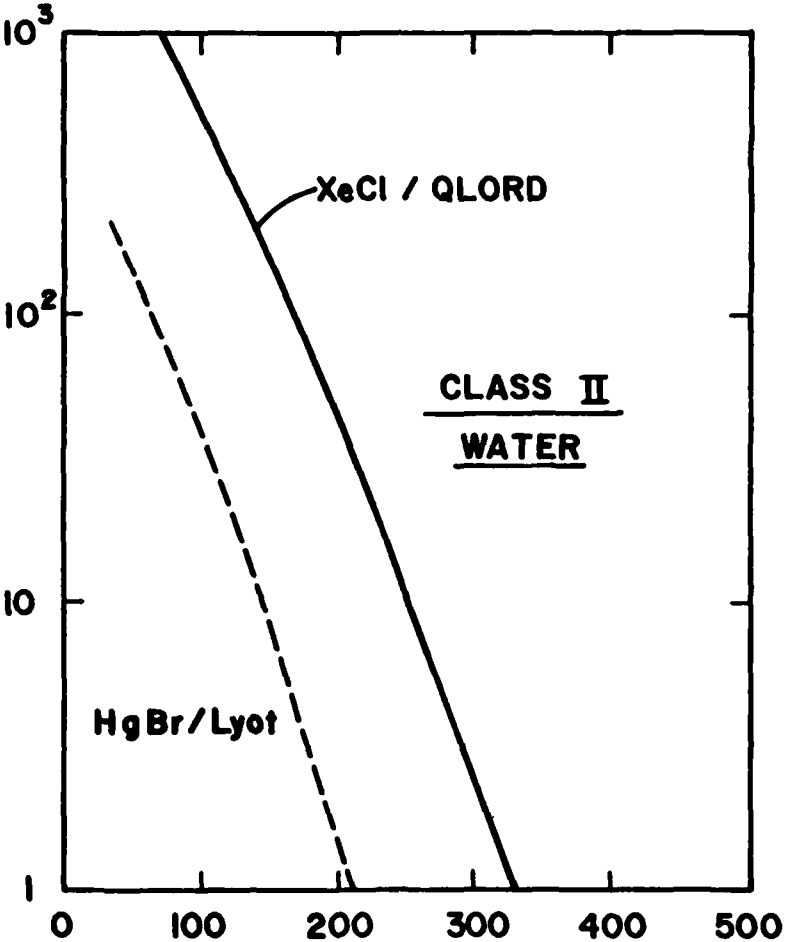

FIGURE 1B

COMPARISON OF SIGNAL-TO-NOISE RATIO FOR XeCl / Raman / QLORD AND HgBr / Lyot - Filter SYSTEMS

FIGURE 1

FIGURE 2 - ENERGY FLOW DIAGRAM FOR ELECTRIC DISCHARGE EXCITED EXCIMER LASER

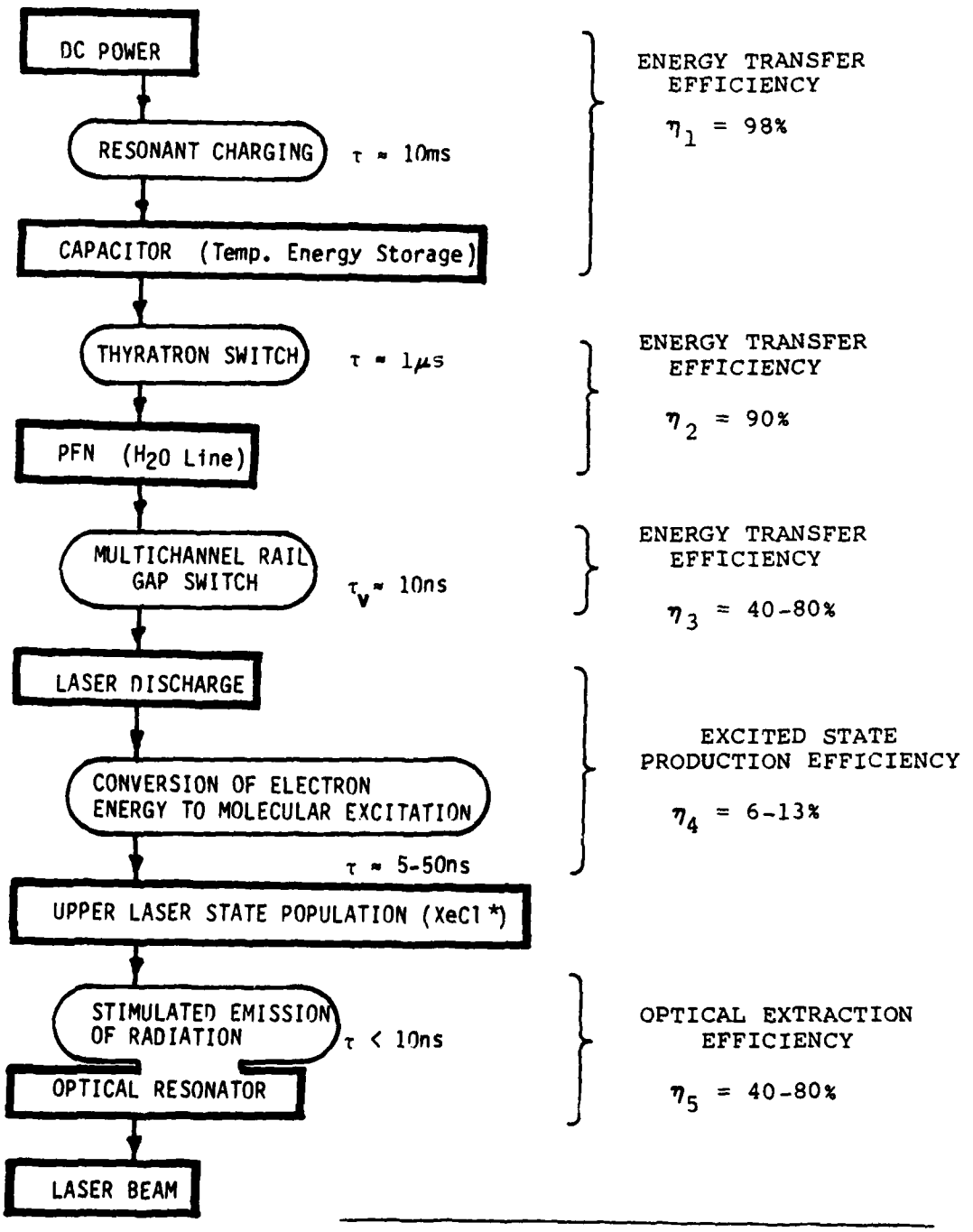

LASER EFFICIENCY

$$\eta = \overline{\prod_i \eta_i} = 0.008 \rightarrow 0.07$$

FIGURE 3

MISMATCHED DOUBLE BLUMLEIN DRIVE

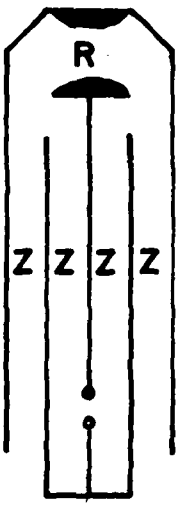

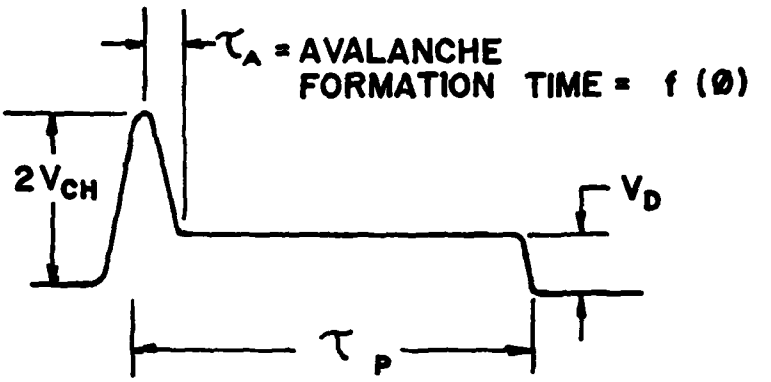

VOLTAGE AT ELECTRODES AS FUNCTION OF TIME

DEFINE "VOLTAGE RATIO" $\emptyset \equiv \frac{2V_{CH}}{V_D}$

FOR IMPEDANCE-MATCHED CONDITION:

$\emptyset = 2$, $Z = R = V_D^2 / P$, $V_D = V_{CH}$

FOR $\emptyset > 2$, $Z > R$, $V_D < V_{CH}$

ENERGY TRANSFER EFFICIENCY (NEGL. SWITCH LOSSES):

$$\eta_3 = \frac{U}{U_{PFN}} = \frac{P\tau_P}{\frac{1}{2} CV_{CH}^2} = \frac{4}{\emptyset^2} \frac{Z}{R}$$

$$\boxed{\frac{Z}{R} = \emptyset - 1} \quad , \quad \boxed{\eta_3 = \frac{4(\emptyset - 1)}{\emptyset^2}}$$

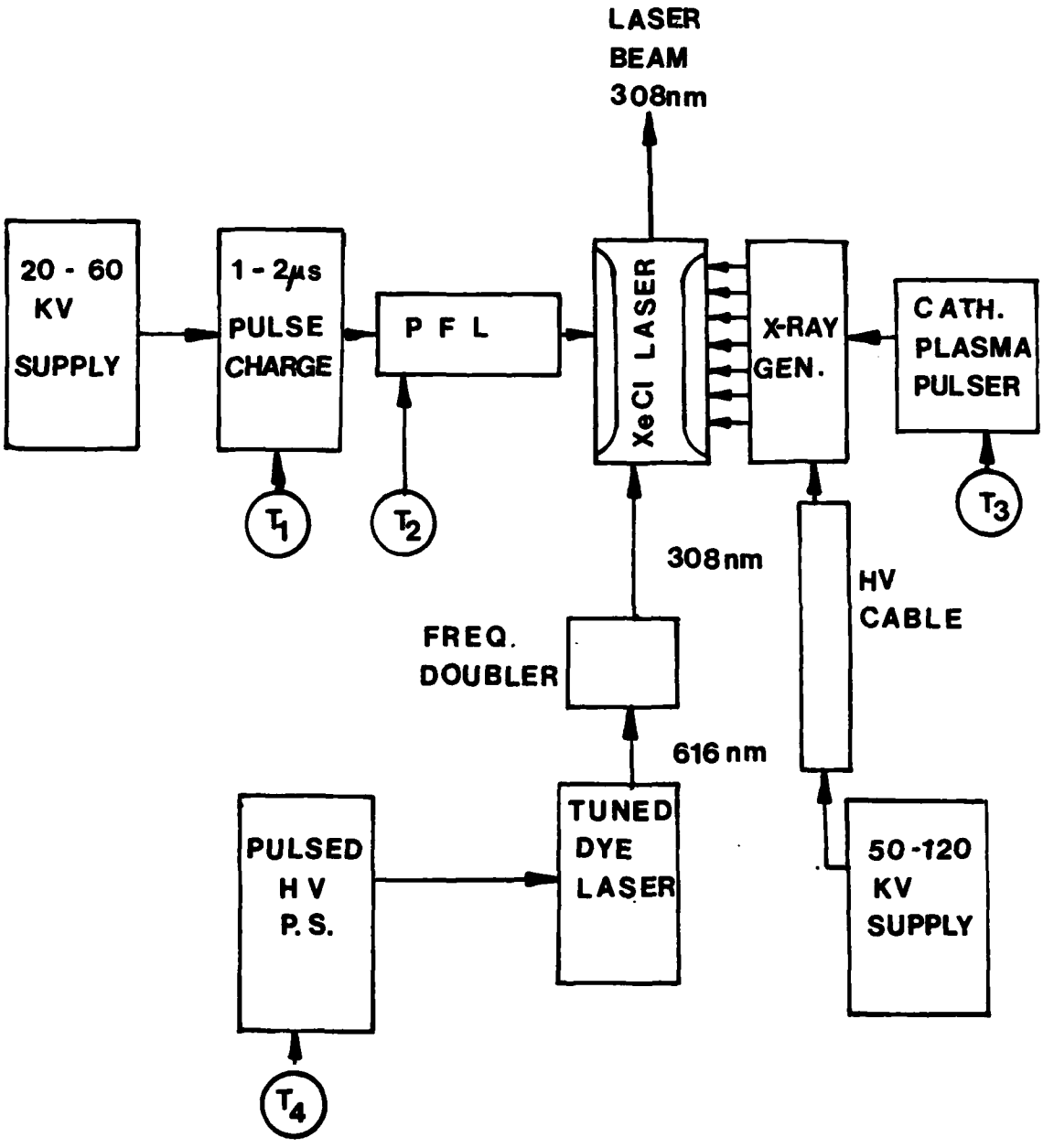

FIGURE 4

EXPERIMENTAL ARRANGEMENT

FIGURE 5

CROSS SECTION THROUGH DISCHARGE CHAMBER

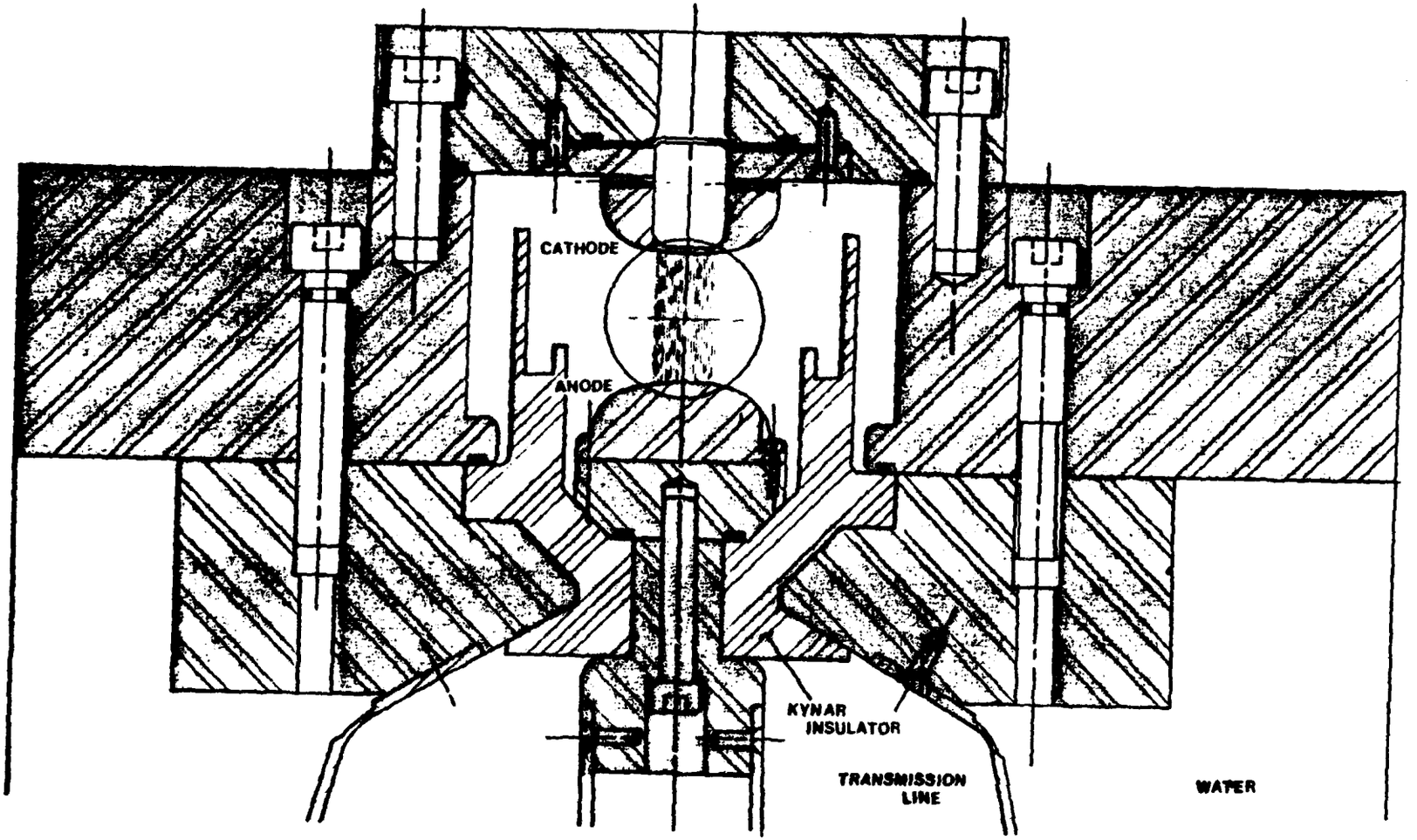

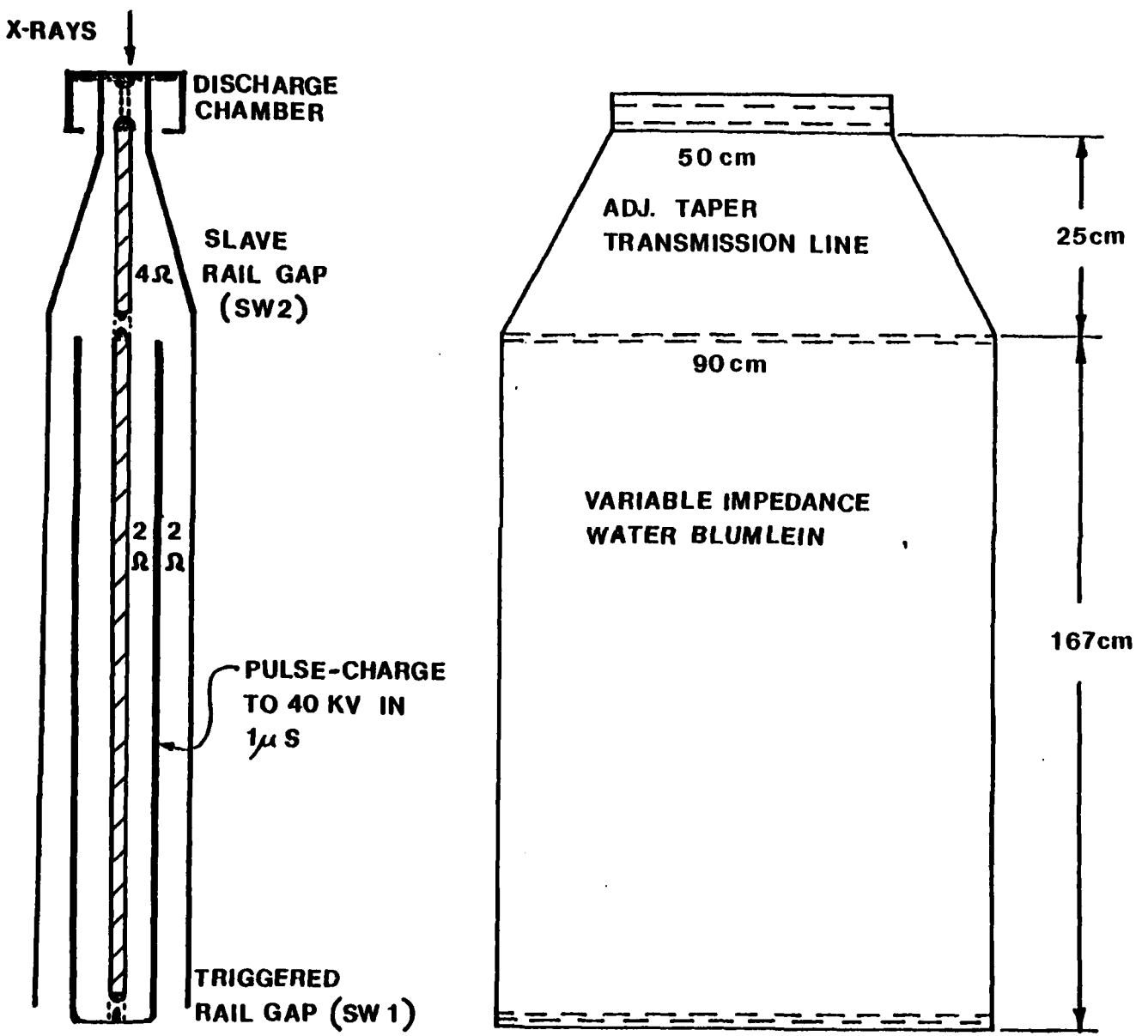

FIGURE 6 GEOMETRY OF PULSE-FORMING NETWORK

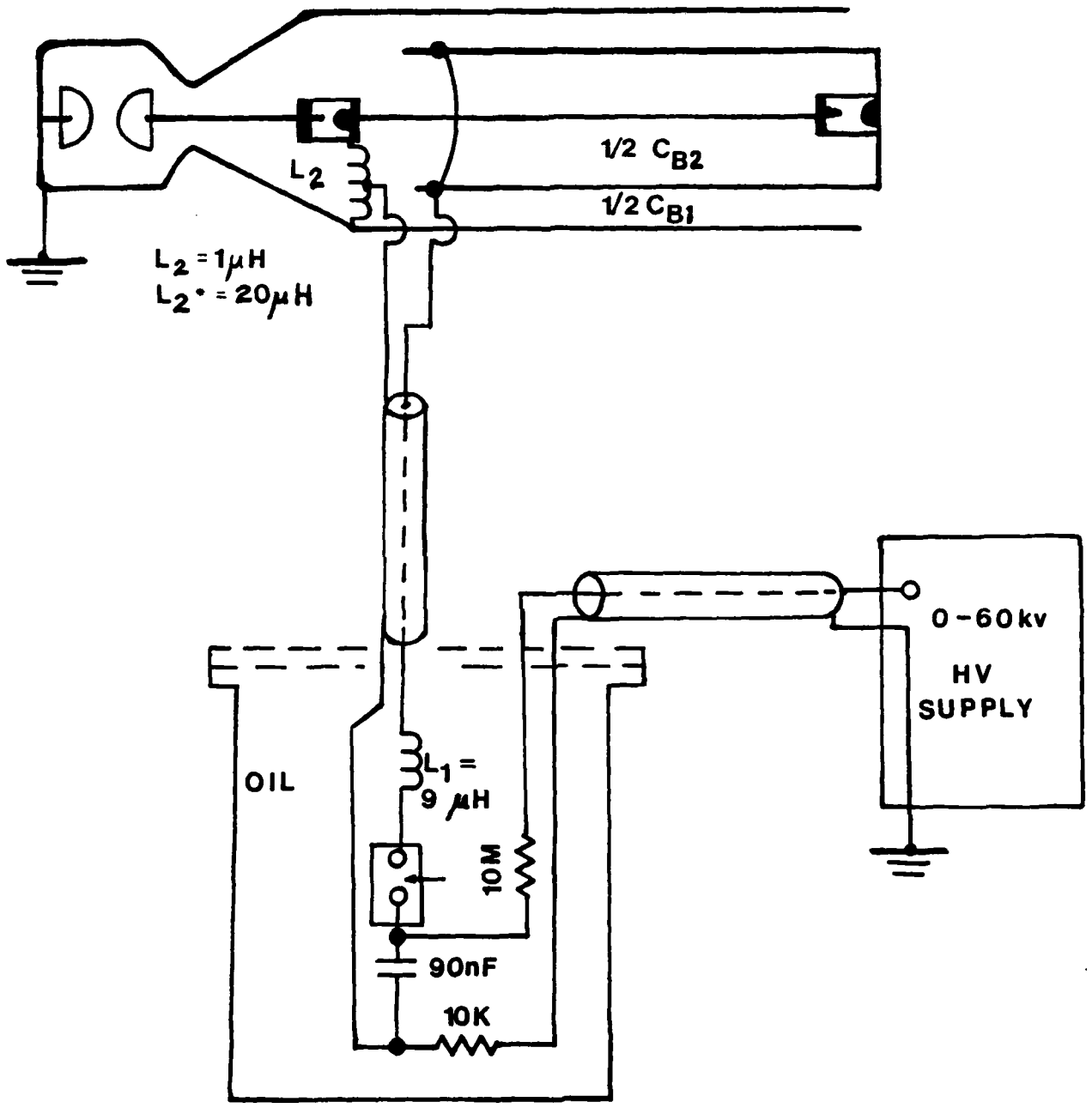

FIGURE 7

SCHEMATIC OF ELECTRIC PULSER

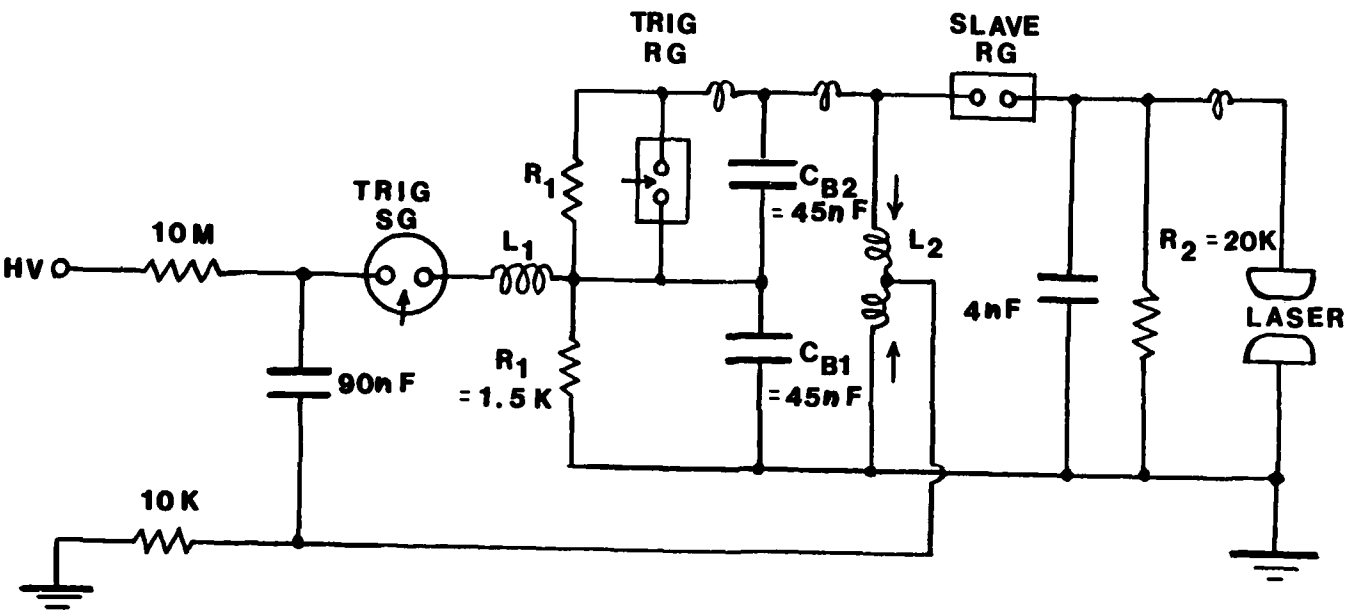

FIGURE 8

"EQUIVALENT" CIRCUIT OF PULSER

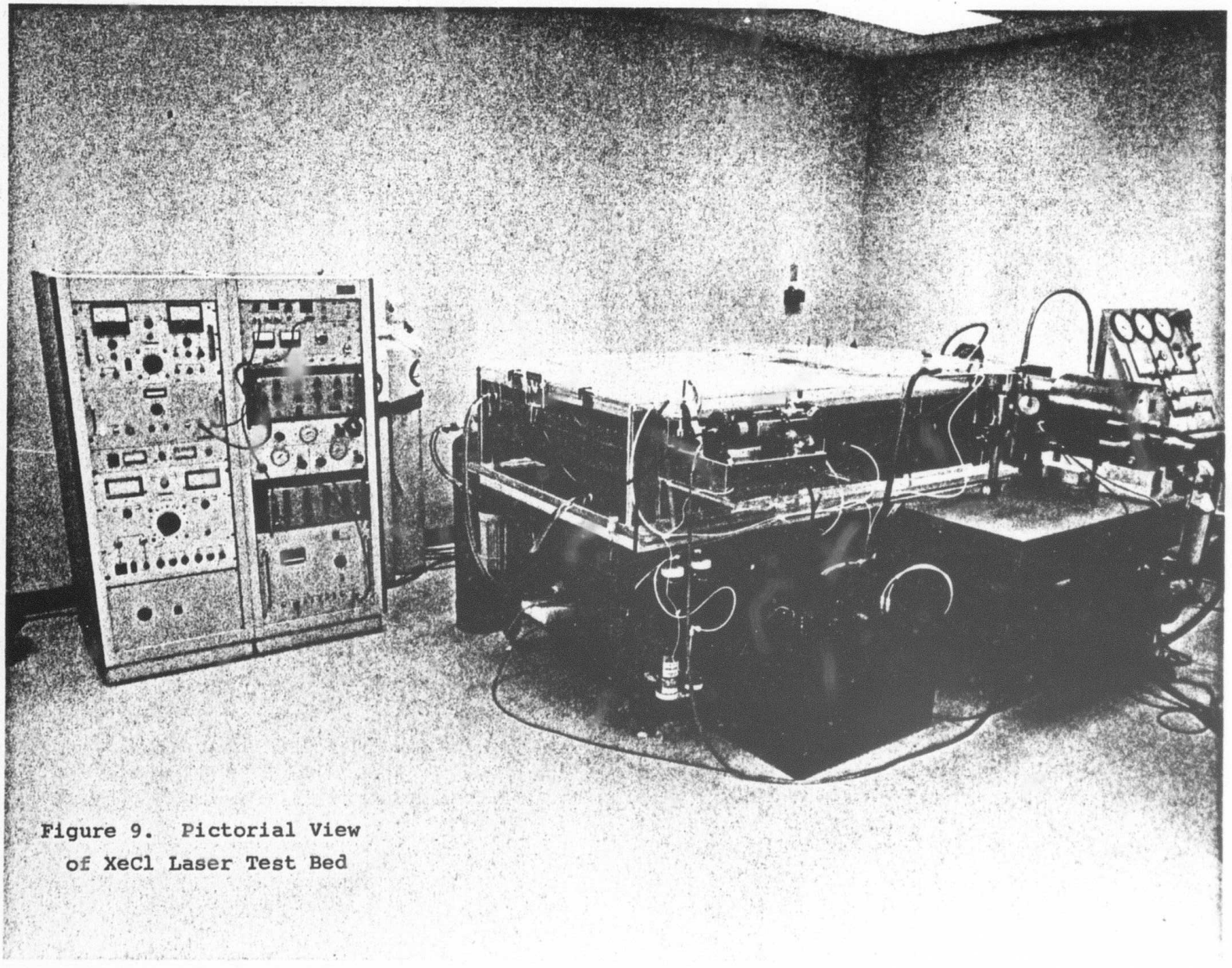

Figure 9. Pictorial View
of XeCl Laser Test Bed

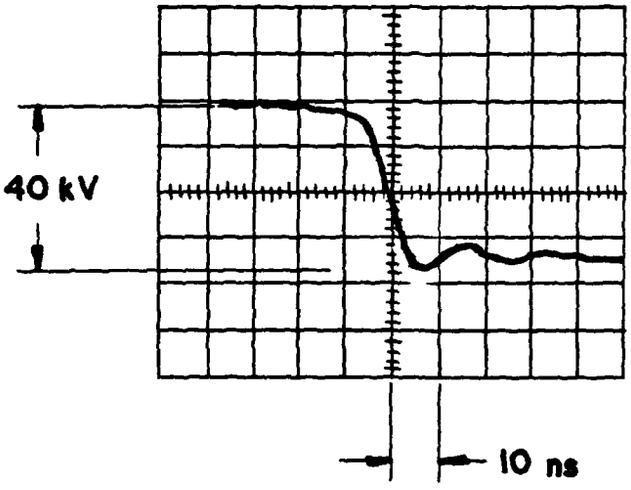

(A)
TRIGGERED
MODE

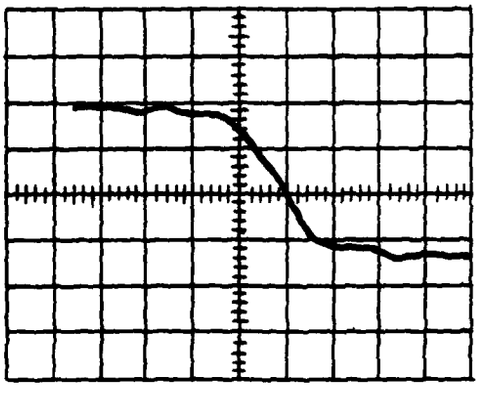

(B)
SELF -
BREAKDOWN
MODE

FIGURE 10. VOLTAGE FALL ACROSS TRIGGERED RAIL GAP

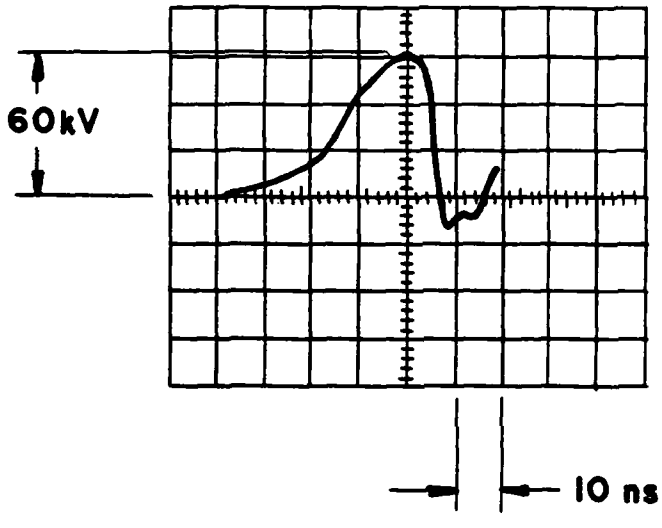

FIGURE 11. VOLTAGE ACROSS SLAVE RAIL GAP

TABLE 1

APPROACHES FOR IMPROVING THE EFFICIENCY OF XeCl LASER

APPROACH	POSSIBLE IMPROVEMENT FACTOR *
1. MAXIMIZE ENERGY TRANSFER FROM PFN TO DISCHARGE	1.90
2. OPTIMIZE LASER KINETICS	1.44
3. MINIMIZE OPTICAL EXTRACTION LOSSES	1.43

* BASED ON BASELINE EFFICIENCY OF 2.1 % OBTAINED BY NRTC IN 1981 ($\eta_3 \approx 0.42, \eta_4 \approx 0.09, \eta_5 \approx 0.56$)

TABLE 2 —

MAXIMIZE ENERGY TRANSFER FROM PFN TO DISCHARGE

TECHNIQUE	MEANS OF OPTIMIZATION	DESIGN CONSIDERATIONS
1A. MATCH PFN AND DISCHARGE IMPEDANCES	• Large Discharge & Line Impedances	• Large Electrode Separation • High Voltage → High Pressure • Moderate Pump Power (<1GW) • P= 6 to 10 atm for Ne
1B. MINIMIZE PUMP-POWER BUILD-UP LOSSES	• Fast di/dt • Long Pulse Duration (>50ns)	• Small Discharge-Chamber Section (Low L) • High Line Impedance • Use of Double Transmission Lines
1C. MAXIMIZE DISCHARGE STABILITY	• Fast dV/dt	• Short Resistive and Inductive Phases of Switch Closure • Large No. of Spark Channels • Low Switch Inductances (Long Spark Gap Rails) • 2nd Pulse-Sharpening Gap • Tapered Transmission Line
	• Uniform Preionization	• X-Ray Preionization
	• Current-Limiting PFN	• Transmission Line and/or Blumlein
1D. MINIMIZE SWITCH LOSSES	• Short Resistive Phase	• Large No. of Spark Channels • Low Line Impedance • Fast dV/dt On Slave Gap • High Pressure H_2 Instead of Air
	• Large Line Impedance	

TABLE 3 -

OPTIMIZATION OF KINETICS AND OPTICAL CAVITY

APPROACH	MEANS OF OPTIMIZATION	DESIGN CONSIDERATIONS
2. OPTIMIZE LASER KINETICS	● High Pump Power Density ● High Pressure Neon Mixture	● Small Discharge Volume ● High Voltage ● Moderate Pulse Length (<100ns)
	● Use of Gas Mixtures Which Raise E/N & Electron Energy In Discharge	● Maximize Discharge Stability
3. MINIMIZE OPTICAL EXTRACTION LOSSES	● Speed Up Optical Oscillation Build-Up	● Injection Lock ● Short Cavity (<1m) ● Short Pump-Power Build-Up
	● Eliminate Parasitic Modes	● Moderate Optical Gain ● Rough Electrodes

TABLE 4

AVALANCHE FORMATION TIME

FOR TYPICAL XeF LASER MIXTURE e-FOLDING TIME
(LUO , 1978)

τ = 2.5 ns FOR $\emptyset$ = 2

τ = 0.6 ns FOR $\emptyset$ = 3

τ = 0.3 ns FOR $\emptyset$ = 4

PREIONIZATION LEVEL $n_e \approx 10^8$ cm^{-3}

ELECTRON NUMBER DENSITY IN DISCHARGE $n_e \approx 10^{14}$ cm^{-3}

INCREASE IN n_e CORRESPONDS TO 14 e-FOLDINGS

$\emptyset$	τ_A	η_3
2	35 ns	1.00
3	8 ns	0.89
4	4 ns	0.75

DESIGN FOR $\emptyset$ = 3

TABLE 5

XeCl LASER DESIGN PARAMETERS

OPTICAL BEAM ENERGY	$U_o = 2J$
EFFICIENCY	$\eta_L = 3\%$
ELECTRICAL ENERGY STORED	$U_{PFN} = 75J$
ELECTRICAL POWER INTO DISCHARGE	$p = 0.7$ GW
PULSE DURATION	$\tau_p = 100$ ns
VOLTAGE RATIO	$\phi = 2V_{CH}/V_D = 3$
DISCHARGE VOLTAGE	$V_D = 27$ kV
CHARGE VOLTAGE	$V_{CH} = 40.5$ kV
TYPICAL GAS MIXTURE	Ne/Xe/HCl = 97.8/2/0.2
GAS PRESSURE	$p = 6$ atm
DISCHARGE FIELD	$E/p = 1.25$ kV/cm-atm $E/N = 4.7 \times 10^{-17}$ V-cm^2
DISCHARGE VOLUME	$\upsilon = d \times w \times l$ $= 3.6 \times 1.8 \times 50$ $= 324$ cm^3
ENERGY DENSITY	$U/\upsilon = 200$ J/l $U/\upsilon p = 35$ J/l-atm
PUMP POWER DENSITY	$P/\upsilon = 2.0$ MW/cm^3
DISCHARGE IMPEDANCE	$R = V_D^2/P = 1.1\Omega$
TRANSMISSION LINE IMPEDANCE	$Z = (\phi - 1)R = 2R = 2.2\Omega$